

***CP*-violating phenomenological MSSM**

Joshua Berger,<sup>1,2,\*</sup> Matthew W. Cahill-Rowley,<sup>1,†</sup> Diptimoy Ghosh,<sup>3,4,‡</sup> JoAnne L. Hewett,<sup>1,§</sup>  
Ahmed Ismail,<sup>5,6,||</sup> and Thomas G. Rizzo<sup>1,¶</sup>

<sup>1</sup>*SLAC National Accelerator Laboratory, 2575 Sand Hill Road, Menlo Park, California 94025, USA*

<sup>2</sup>*Department of Physics, University of Wisconsin, Madison, Wisconsin 53766, USA*

<sup>3</sup>*INFN, Sezione di Roma, Piazzale A. Moro 2, I-00185 Roma, Italy*

<sup>4</sup>*Department of Particle Physics and Astrophysics, Weizmann Institute of Science, Rehovot 7610001, Israel*

<sup>5</sup>*Argonne National Laboratory, 9700 South Cass Avenue, Argonne, Illinois 60439, USA*

<sup>6</sup>*University of Illinois at Chicago, 845 West Taylor Street, Chicago, Illinois 60607, USA*

(Received 22 November 2015; published 16 February 2016)

We investigate the sensitivity of the next generation of flavor-based low-energy experiments to probe the supersymmetric parameter space in the context of the phenomenological minimal supersymmetric Standard Model and examine the complementarity with direct searches for supersymmetry at the 13 TeV LHC in a quantitative manner. To this end, we enlarge the previously studied phenomenological minimal supersymmetric Standard Model parameter space to include all physical nonzero *CP*-violating phases, namely those associated with the gaugino mass parameters; Higgsino mass parameter and the trilinear couplings of the top quark, bottom quark, and tau lepton. We find that future electric dipole moment and flavor measurements can have a strong impact on the viability of these models even if the sparticle spectrum is out of reach of the 13 TeV LHC. In particular, the lack of positive signals in future low-energy probes would exclude values of the phases between  $\mathcal{O}(10^{-2})$  and  $\mathcal{O}(10^{-1})$ . We also find regions of parameter space where large phases remain allowed due to cancellations. Most interestingly, in some rare processes, such as  $\text{BR}(B_s \rightarrow \mu^+ \mu^-)$ , we find that contributions arising from *CP*-violating phases can bring the potentially large supersymmetry contributions into better agreement with experiment and Standard Model predictions.

DOI: [10.1103/PhysRevD.93.035017](https://doi.org/10.1103/PhysRevD.93.035017)

**I. INTRODUCTION**

The virtual effects of new interactions provide an important window of opportunity to probe the presence of physics beyond the Standard Model (SM). In particular, measurements of flavor-changing and *CP*-violating processes yield stringent tests of the SM at the quantum loop-level [1–6] and are potentially sensitive to new physics (NP) at scales far beyond the reach attainable at colliders in the foreseeable future. For example, constraints on new contributions to the four-quark operators that mediate neutral meson mixing place severe bounds on a NP scale of up to  $10^{3-5}$  TeV for unit coupling strength. Alternatively, if new interactions are present at the TeV scale, these limits constrain the effective coupling strength to be below  $10^{-11}$  to  $10^{-5}$  [1].

The power of low-energy measurements in constraining UV-complete theories is best illustrated by the strong limit on sfermion masses in supersymmetry (SUSY) theories [7–11]. In particular, the *CP*-conserving and *CP*-violating observables in meson mixing, together with constraints on the electric dipole moment (EDM) of the neutron and electron,

exclude TeV-scale SUSY-breaking parameters if the *CP*-violating phases and sfermion mixing angles are of order 1 [12–16]. For example, constraints from neutral kaon mixing require squarks to be heavier than  $\sim 500$  TeV if the squark mass matrices have an anarchic flavor structure. Clearly, a viable model of TeV-scale supersymmetry requires a specific flavor structure to accommodate the data; such structures are in fact present in many specific models of SUSY breaking [17–20]. Despite the necessary presence of a flavor structure that suppresses supersymmetric contributions to experimental observables, next-generation flavor experiments will be sensitive to TeV-scale SUSY, as the mechanisms suppressing flavor and *CP* violation are not completely effective at the level of expected experimental sensitivity. In addition, if supersymmetry is discovered via direct production at the LHC, then measurements in the flavor sector will be essential to determine the flavor structure of the underlying theory. Conversely, flavor experiments may provide a discovery path, having sensitivity to TeV-scale SUSY scenarios that are difficult to observe at the LHC. It is thus imperative to perform a comprehensive analysis to examine the sensitivity of future flavor experiments to terascale supersymmetry and compare that to expectations for Run II at the LHC.

In order to be inclusive and avoid prejudice on the modelling of physics at the high scale, we examine terascale SUSY in a general framework that captures the phenomenology of a variety of SUSY-breaking models, as

\*jberger@slac.stanford.edu

†mrowley@slac.stanford.edu

‡diptimoy.ghosh@weizmann.ac.il

§hewett@slac.stanford.edu

||aismail@anl.gov

¶rizzo@slac.stanford.edu

well as that of SUSY-breaking mechanisms which remain to be discovered. We thus consider the phenomenological minimal supersymmetric Standard Model (pMSSM) [21,22], a subspace of the minimal supersymmetric Standard Model (MSSM) designed to examine regions of parameter space that have been unexplored in studies of more simplified models. The pMSSM is constructed from the general R-parity-conserving MSSM by imposing the following set of data-driven assumptions: (i) no new sources of  $CP$  violation, (ii) minimal flavor violation at the electroweak scale so that flavor violation is proportional to the CKM mixing matrix elements, (iii) degenerate first and second generation sfermion masses, and (iv) negligible Yukawa couplings and  $A$ -terms for the first two generations. This results in a 19-dimensional parameter space, containing ten scalar masses; three gaugino masses,  $M_{1,2,3}$ ; the three third generation  $A_{t,b,\tau}$ -terms; and three parameters related to the SUSY Higgs potential,  $\mu$ ,  $M_A$ , and  $\tan\beta$ .

In order to examine the pMSSM contributions to  $CP$ -violating observables in this study, we augment the parameter space to include nonzero  $CP$ -violating phases. Including nonvanishing  $CP$  phases is particularly interesting because of their possible role in baryogenesis, as well as their potential to slightly increase the predicted value of the light Higgs mass within SUSY [23]. In particular,  $CP$ -violating phases can relieve some of the tension between the requirement of heavy stops and/or large stop mixing needed to generate the observed Higgs mass vs the light stops and small mixing preferred by naturalness. Specifically, we explore the effect of including all six  $CP$ -violating phases that are consistent with the pMSSM assumption of minimal flavor violation:  $\phi_1 \equiv \arg(M_1)$ ,  $\phi_2 \equiv \arg(M_2)$ ,  $\phi_\mu \equiv \arg(\mu)$ ,  $\phi_t \equiv \arg(A_t)$ ,  $\phi_b \equiv \arg(A_b)$ , and  $\phi_\tau \equiv \arg(A_\tau)$ . We then study the effects of these nonzero phases on a variety of  $CP$ -conserving and  $CP$ -violating processes. We find that flavor observables place important constraints on the allowed soft SUSY-breaking parameters, despite the assumptions ii–iv listed above. Interestingly, in some rare processes, such as  $\text{BR}(B_s \rightarrow \mu^+\mu^-)$ , we find that the inclusion of  $CP$  phases can have the effect of bringing the SUSY contributions more in line with SM expectations, and hence in better agreement with experiment. We will see that flavor constraints on the  $CP$ -extended pMSSM provide an additional handle that could allow SUSY to be discovered by the next generation of low-energy experiments, even if the sparticle spectrum is out of kinematic reach at the LHC. Such low-energy experiments are thus seen as complementary to the direct LHC SUSY searches in a manner similar to both the direct and indirect searches for dark matter [24]. This work expands upon the Snowmass study presented in Ref. [25].

## II. ANALYSIS PROCEDURE

For this study, we extend the  $CP$ -conserving pMSSM model sample produced in Ref. [26] which contains a

TABLE I. Scan ranges for the 25 parameters of the phase-extended pMSSM with a neutralino LSP. Mass parameters and  $\tan\beta$  are scanned with flat priors, while the phases are scanned with log priors.

$m_{\tilde{L}(e)_{1/2,3}}$	100 GeV–4 TeV
$m_{\tilde{Q}(u,d)_{1/2}}$	400 GeV–4 TeV
$m_{\tilde{Q}(u,d)_3}$	200 GeV–4 TeV
$ M_1 $	50 GeV–4 TeV
$ M_2 $	100 GeV–4 TeV
$ \mu $	100 GeV–4 TeV
$M_3$	400 GeV–4 TeV
$ A_{t,b,\tau} $	0 GeV–4 TeV
$M_A$	100 GeV–4 TeV
$\tan\beta$	1–60
$\phi_1$	$(10^{-6}-1)\frac{\pi}{2}$
$\phi_2$	$(10^{-6}-1)\frac{\pi}{2}$
$\phi_\mu$	$(10^{-6}-1)\frac{\pi}{2}$
$\phi_t$	$(10^{-6}-1)\frac{\pi}{2}$
$\phi_b$	$(10^{-6}-1)\frac{\pi}{2}$
$\phi_\tau$	$(10^{-6}-1)\frac{\pi}{2}$

neutralino lightest supersymmetric particle (LSP). This sample corresponds to a set of models (i.e., points in the parameter space), generated by a random scan employing flat priors over the 19 pMSSM parameters. The scan ranges, shown in Table I, were selected to enable phenomenological studies at the 14 TeV LHC. These models were subjected to a global set of collider, flavor, precision electroweak, dark matter, and theoretical constraints. We note that the WMAP/Planck measurement of the dark matter relic density was only employed as an upper bound, so that the LSP need not saturate this value, allowing for the possibility of multicomponent dark matter. This procedure generated  $\sim 225$  k pMSSM models that can be adopted for further studies. The signatures of this model sample at the 7, 8, and 14 TeV LHC were recently examined in Ref. [27] using a fast Monte Carlo simulation of the ATLAS SUSY analysis suite. In that work, the expected ability of ATLAS to observe each model for each center-of-mass energy was determined.<sup>1</sup> In particular, it was found that models with light squarks and gluinos remain viable after the LHC Run I at 7 and 8 TeV. These collider results will enable the comparison of the discovery reach between direct searches at the 14 TeV LHC and indirect effects in future low-energy precision measurements.

To extend this previous study to include  $CP$ -violating phases, we choose a random subset of 1000 models from this large pMSSM model sample which survive the 7 and 8 TeV LHC searches, ensuring that each model is in agreement with the observed Higgs mass within 3 GeV,

<sup>1</sup>We note that our projections for the sensitivity of the 14 TeV LHC to the pMSSM models under consideration include only the search channels expected to be the most powerful.

TABLE II. List of model categories referred to in the text along with the number of models in the category and a brief description. For further details, see the text.

Set name	No of models	Description
A	1000	Full pMSSM model set without phases
A1	500	pMSSM models to which LHC-14 will be sensitive
A2	500	pMSSM models which evade LHC-14 constraints
B	$10^6$	Full model set A extended to include random phases
B1	$5 \times 10^5$	A1 with random phases
B2	$5 \times 10^5$	A2 with random phases
C	155, 474	Number from set B allowed by current flavor $CP$ constraints
C1	75, 216	Number from B1 allowed by current flavor $CP$ constraints
C2	80, 258	Number from B2 allowed by current flavor $CP$ constraints
D	3708	Number from set B allowed after future flavor $CP$ null results
D1	1714	Number from B1 allowed after future flavor $CP$ null results
D2	1994	Number from B2 allowed after future flavor $CP$ null results

corresponding to the theoretical error on the prediction of the Higgs mass in supersymmetry [28]. These models have the following characteristics: half of these models (i.e., 500 models) are predicted to be detectable at the 14 TeV LHC with  $300 \text{ fb}^{-1}$ , while the other half are expected to remain viable (i.e., unobserved) even after  $3000 \text{ fb}^{-1}$  at 14 TeV as described in Ref. [27]. Since the  $CP$ -violating phases have a minimal impact on the observability of models at the LHC, we choose to consider the effect of incorporating  $CP$ -violating phases to pMSSM models for which the LHC phenomenology has already been studied.

We now extend the 19-dimensional parameter space of each of these 1000 pMSSM models to include the phases present in the MSSM that are consistent with the pMSSM flavor structure. As discussed above, generically, six combinations of MSSM parameters can take on physical  $CP$ -violating phases; these combinations can be chosen to be  $M_1\mu B_\mu^*$ ,  $M_2\mu B_\mu^*$ ,  $M_3\mu B_\mu^*$ ,  $A_t M_3^*$ ,  $A_b M_3^*$ , and  $A_\tau M_3^*$ . We choose to work in a basis where  $M_3$  and  $B_\mu$  are real, so that the parameters with physical phases are  $M_1$ ,  $M_2$ ,  $\mu$ ,  $A_t$ ,  $A_b$ , and  $A_\tau$ . For each of the 1000 models, we perform a random scan over these six physical phases, generating an additional 1000 models in each case, resulting in a total of  $10^6$  models with  $CP$ -violating phases. The scan over the phases incorporates a log-uniform distribution over the range  $10^{-6}\pi/2$  to  $\pi/2$ , with a random sign, as summarized in Table I. This choice facilitates the study of a wider range of possible phases than that obtainable with a simple uniform scan distribution. The overall sign of the parameters corresponding to these phases is fixed in the pMSSM. The choice of a  $\pi/2$  upper bound on the magnitude of the phase preserves the sign of the real part of the corresponding parameters. To restate, the result of this scan yields a total of 1 million models with nonzero  $CP$ -violating phases available for study.

In what follows, we will refer to several different categories of models within our  $10^6$  model sample of the phase-extended pMSSM. For clarity and ease of

reference, the various model subcategories considered in this work are summarized in Table II. The original 1000 pMSSM models without phases are denoted as set A, divided into the half that is observable at the 14 TeV LHC (A1) and the half that is expected to evade the 14 TeV SUSY searches (A2). The full set of  $10^6$  models in the phase-extended pMSSM is designated as set B. B1 (B2) refers to the phase-extended models that are derived from the zero-phase pMSSM A1 (A2) models that are observable (not observable) at the 14 TeV LHC, as detailed above.

In this study, we employ the `SUSY_FLAVOR v2.10` code [29–31] to calculate a comprehensive set of low-energy observables for the  $10^6$  models in set B. We performed an extensive number of analyses to verify the consistency of the output of the `SUSY_FLAVOR v2.10` code. The full list of processes we study is given in Table III, along with the SM prediction for each observable as calculated by `SUSY_FLAVOR`, the current experimental result, and the expected future experimental plus theory uncertainties or bounds as applicable. We note that in many cases, the expected future measurements will provide a vast improvement over current sensitivity. The values of the input parameters, and their sources, that are required for the `SUSY_FLAVOR` computations are listed in Table IV. Where they overlap, we took the input parameters to be identical to those used to generate the corresponding pMSSM models. The remaining parameters were chosen according to recent measurements, global data fits, or lattice calculations.

The observables listed in Table III are the most constraining flavor- and  $CP$ -violating processes computed by `SUSY_FLAVOR`. While the focus of this work is on  $CP$ -violating observables, the addition of  $CP$ -violating phases can also modify the pMSSM predictions for flavor changing,  $CP$ -conserving transitions due to the presence of  $\phi$ -dependent terms in the overall rates. Furthermore, only some of the low-energy constraints in Table III have been applied during the generation of the pMSSM models in previous studies [26]. The constraints from these processes

TABLE III. The complete set of observables studied in this work. All processes are computed using SUSY\_FLAVOR v2.10.

Observable	SM	Experiment <sup>a</sup>	Future theory $\oplus$ Experiment bound/uncertainty
$ d_e $ (e · cm)	$\lesssim \mathcal{O}(10^{-40})$ [32,33]	$< 8.7 \times 10^{-29}$ [34]	$\lesssim 10^{-30}$ [1,35,36]
$ d_\mu $ (e · cm)	$\lesssim \mathcal{O}(10^{-38})$ [37]	$< 1.6 \times 10^{-19}$ [38]	$\lesssim 10^{-24}$ [1,39]
$ d_n $ (e · cm)	$\lesssim \mathcal{O}(10^{-31})$ [40,41]	$< 2.9 \times 10^{-26}$ [42]	$\lesssim 5 \times 10^{-28}$ [43]
$a_e$ [ $10^{-12}$ ]	$1159652182.79 \pm 7.71$ [44]	$1159652180.73 \pm 28$ [45]	...
$a_\mu$ [ $10^{-11}$ ]	$116591802 \pm 49$ [46] $116591828 \pm 50$	$116592089 \pm 63$ [47]	$\pm 12$ [1]
$\text{Br}(K_L \rightarrow \pi^0 \nu \bar{\nu})$	$3.04 \pm 15.7\% \times 10^{-11}$ [48]	$< 2.6 \times 10^{-8}$ [49]	$\pm 6.0\% \pm 5.1\% = 79\%$ [1,50]
$\text{Br}(K^+ \rightarrow \pi^+ \nu \bar{\nu}) \times 10^{11}$	$9.2 \pm 8.2\%$ [48]	$17.3_{-10.5}^{+11.5}$ [51]	$\pm 5.4\% \pm 2.2\% = 5.8\%$ [1,52]
$\text{Br}(B_d \rightarrow X_s \gamma) \times 10^{4b}$	$3.17 \pm 7.3\%$ [53]	$3.43 \pm 6.7\%$ [54]	$\pm 6.7\% \pm 4.0\% = 7.8\%$ [55]
$\text{Br}(B_s \rightarrow \mu^+ \mu^-) \times 10^9$	$3.74 \pm 4.1\%$ [56]	$2.9 \pm 0.7$ [57]	$\pm 3.2\% \pm 8.6\% = 9.2\%$ [58]
$\text{Br}(B_d \rightarrow \mu^+ \mu^-) \times 10^{10}$	$1.21 \pm 6.1\%$ [56]	$3.6_{-1.4}^{+1.6}$ [57]	$\pm 3.9\% \pm 36.0\% = 36.2\%$ [58]
$\text{Br}(B_u \rightarrow \tau \nu_\tau) \times 10^4$	$0.779 \pm 8.6\%$ [59]	$1.14 \pm 0.22$ [54]	$\pm 6.0\% \pm 6.3\% = 8.7\%$ [55]
$\Delta M_{B_d}$ (ps <sup>-1</sup> )	$0.545 \pm 16.8\%$ [60]	$0.507 \pm 0.005$ [54]	$\pm 3.7\% \pm 0.9\% = 3.8\%$
$\Delta M_{B_s}$ (ps <sup>-1</sup> )	$17.70 \pm 15.0\%$ [60]	$17.719 \pm 0.043$ [54]	$\pm 3.1\% \pm 0.2\% = 3.1\%$
$\Delta M_K (10^{-3} \text{ ps}^{-1})$	4.824	$5.292 \pm 0.009$ [61]	...
$\epsilon_K [10^{-3}]$	$2.319 \pm 9.3\%$ [62]	$2.228 \pm 0.011$ [61]	...
$\sin(2\beta)$	$0.695 \pm 5.6\%$ [62]	$0.68 \pm 0.02$ [54]	$\pm 2.1\% \pm 1.2\% = 2.4\%$ [58]
$\sin(2\beta_s)$	$0.0375 \pm 4.0\%$ [62]	$-0.04_{-0.10}^{+0.13}$ [54]	$\pm 2.5\% \pm 15.8\% = \pm 16.0\%$ [58]

<sup>a</sup>All upper bounds are at 90% C.L.  
<sup>b</sup> $E_\gamma > 1.6$  GeV in the  $B$ -meson rest frame.

offer a more complete picture of the current low-energy restrictions on the pMSSM.

Beginning with the original set B of  $10^6$  models, we first determine the subset of these models that satisfy all of the existing flavor and  $CP$  constraints: We call this set C. Similarly, beginning with the B1 (B2) set, we derive those denoted as C1 (C2). Finally, we also consider the subset of B models that are expected to survive the *future* flavor and  $CP$  constraints according to our study below and refer to that subset as set D with analogously defined D1 and D2 subsets.

In the following analysis, we will mainly investigate model set C, containing the 155,474 models for which the predicted values of the observables in Table III are below the current 90% C.L. limits or within  $2\sigma$  of the observed values for measured quantities.<sup>2</sup> Some models, particularly those with large values of  $\tan\beta$ , can generate significant corrections to the CKM matrix elements, as well as Yukawa couplings [15]. In these cases,  $\tan\beta$  enhancements compensate for loop factor suppressions and can lead to large loop contributions with diminished perturbative control without, e.g., resummation. Thus, we enforce a cut of 40% on the size of the maximal correction to the CKM matrix elements or the Yukawa couplings in model set C, to ensure that perturbative control of the flavor calculations is

<sup>2</sup>We do not apply the experimental constraint on  $(g-2)_\mu$  at this stage as it lies  $3.4\sigma$  deviation from the SM prediction. In the following analysis, we will consider the possibility that future measurements observe either the SM prediction, or the current central value, with increased precision.

maintained. Keeping with our previous nomenclature, we define C1 as the 80,258 models obtained by applying the same LHC constraints as for B1 and, correspondingly, C2 as the 75,216 models obtained by applying the same LHC constraints as in B2. The most constraining observables at this stage are  $d_e$ ,  $\text{Br}(B_s \rightarrow \mu\mu)$ , and  $\text{Br}(B \rightarrow s\gamma)$ .

We will also consider the models denoted by D, D1, and D2 that are expected to remain viable after future flavor experiments are performed *assuming* the central measured value agrees with the SM prediction. The D model sets are comprised of 3708, 1994, and 1714 models, respectively, where D1 and D2 represent the sets corresponding to the LHC discovery criteria described above. In this study, we employ the anticipated future experimental uncertainties given in Ref. [1].

For several observables, the improvement in future sensitivity is dominated by the expected reduction in the error associated with the theoretical calculation of the value for the process. To estimate the theoretical errors, we include the uncertainties from both the input parameters and those due to lattice calculations and/or higher order terms in the expansion employed in the calculation. While the present uncertainties on the observables studied in this work are well documented in the literature, we estimated the projected future uncertainties independently.

Specifically, we estimate the future theoretical uncertainties on an observable  $O$  as follows. In general, the calculation of  $O$  can depend on model parameters  $\alpha_i$  which are expected to be determined with uncertainties  $\sigma(\alpha_i)$  with updated experimental input or improved calculations. The most important parameters  $\alpha_i$  for our analysis are the CKM

TABLE IV. Values of Standard Model, lattice, and observational quantities we employ with SUSY\_FLAVOR v2.10.

Observable	Value
pMSSM input	
$\alpha^{-1}(m_Z)$	127.8568 [26]
$\alpha_s(m_Z)$	0.1193 [63]
$m_Z$	91.1876 GeV [61]
$m_W$	80.385 GeV [61]
$m_b(m_b)$	4.16 GeV [64]
$m_t^{\text{pole}}$	173.2 GeV [65]
Quark masses and $D$ -meson mass [61]	
$m_u(2 \text{ GeV})$	2.3 MeV
$m_d(2 \text{ GeV})$	4.8 MeV
$m_s(2 \text{ GeV})$	95 MeV
$m_e$	0.510998928 MeV
$m_\mu$	105.659 MeV
$m_\tau$	1.777 GeV
$m_D$	1.8645 GeV
$\Delta m_D$	$1.56 \times 10^{-14} \text{ GeV}^{-1}$
CKM [6]	
$\lambda$	0.22535
$A$	0.822
$\bar{\rho}$	0.127
$\bar{\eta}$	0.353
Experimental inputs [66]	
$m_c(m_c)$	1.279 GeV
$m_K$	497.614 MeV
$m_{B_d}$	5.2792 GeV
$m_{B_s}$	5.3668 GeV
$\tau_{B_d}$	1.519 ps <sup>-1</sup>
$\tau_{B_s}$	1.516 ps <sup>-1</sup>
$\Delta m_K$	$3.483 \times 10^{-15} \text{ GeV}^{-1}$
$\Delta m_{B_d}$	$3.36 \times 10^{-13} \text{ GeV}^{-1}$
$\Delta m_{B_s}$	$1.164 \times 10^{-11} \text{ GeV}^{-1}$
$\epsilon_K$	$2.228 \times 10^{-3}$
$n$ EDM [29]	
$\eta_e$	1.53
$\eta_c$	3.4
$\eta_g$	3.4
$\Lambda_X$	1.18 GeV
Lattice Averages	
$f_D$	200 MeV

TABLE IV. (Continued)

Observable	Value
Basic lattice parameters [66]	
$f_K$	156.1 MeV
$f_{B_d}$	190.5 MeV
$f_{B_s}$	227.7 MeV
$\eta_{cc}$	1.87
$\eta_{ct}$	0.496
$\eta_{tt}$	0.5765
$\eta_b$	0.55
$\hat{B}_K$	0.766
$\hat{B}_{B_d}$	1.27
$\hat{B}_{B_s}$	1.33
$\kappa_0$	$(2.31 \pm 0.01) \times 10^{-10}$
$\kappa_+$	$(5.36 \pm 0.026) \times 10^{-11}$
$P_c$	$(0.42 \pm 0.03) \times 10^{-10}$
$K$ - and $D$ -meson $B$ [67]	
$B_K^{VLL}(2 \text{ GeV})$	0.52
$B_K^{SLL1}(2 \text{ GeV})$	0.54
$B_K^{SLL2}(2 \text{ GeV})$	0.27
$B_K^{LR1}(2 \text{ GeV})$	0.63
$B_K^{LR2}(2 \text{ GeV})$	0.82
$B_D^{VLL}(2 \text{ GeV})$	0.78
$B_D^{SLL1}(2 \text{ GeV})$	0.71
$B_D^{SLL2}(2 \text{ GeV})$	0.45
$B_D^{LR1}(2 \text{ GeV})$	1.17
$B_D^{LR2}(2 \text{ GeV})$	0.94
$D$ -meson renormalization group-invariant $B$	
$\hat{B}_D$	1.17
$B$ -meson $B$ [68]	
$B_{B_d}^{VLL}(m_b)$	0.85
$B_{B_d}^{SLL1}(m_b)$	0.72
$B_{B_d}^{SLL2}(m_b)$	0.61
$B_{B_d}^{LR1}(m_b)$	1.47
$B_{B_d}^{LR2}(m_b)$	0.95
$B_{B_s}^{VLL}(m_b)$	0.86
$B_{B_s}^{SLL1}(m_b)$	0.73
$B_{B_s}^{SLL2}(m_b)$	0.62
$B_{B_s}^{LR1}(m_b)$	1.57
$B_{B_s}^{LR2}(m_b)$	0.93

angle  $|V_{ub}|$  and the CKM phase  $\delta$ , although we include all the parameters listed in Table IV. The uncertainty in  $O$  due to the corresponding error in  $\alpha_i$  can be estimated as

$$\sigma_i(O) = \frac{\partial O}{\partial \alpha_i} \sigma(\alpha_i). \quad (1)$$

The computation of  $O$  can also have an uncertainty due to the approximations used to derive the amplitude for  $O$ , which we denote by  $\sigma_{\text{th}}(O)$ . Then the total uncertainty  $\sigma(O)$  for an observable can be determined by adding  $\sigma_i(O)$  and  $\sigma_{\text{th}}(O)$  in quadrature as

$$\sigma^2(O) = \sigma_{\text{th}}^2(O) + \sum_i \sigma_i^2(O). \quad (2)$$

Strictly speaking, the theoretical uncertainty is model dependent; however, we assume the SM and leading expressions for  $O$  in our estimations. The uncertainties estimated in this manner are more conservative than those quoted in other studies but generally agree well (see Table III). In order to obtain projections for future uncertainties, we assume the improvements in the model parameters as outlined in Ref. [1], while taking  $\sigma_{\text{th}}(O)$

to remain unchanged. The resulting error projections are shown in the rightmost column of Table III.

It is worth noting already at this point that the relative sizes of the two subsets C1 and C2, as well as D1 and D2, are comparable. This observed similarity is an indicator of a high degree of complementarity between the direct searches at the LHC and low-energy probes of the MSSM. A strong constraint from the LHC only biases the low-energy bounds by roughly  $\sim 10\%$ .

### III. NUMERICAL RESULTS

We now characterize the model sets C and D, the pMSSM models with  $CP$  phases satisfying the current and expected future constraints, respectively, from low-energy observables.

We begin our survey with an overview of the values of the phases in the  $CP$ -violating pMSSM. The first five panels of Fig. 1 contain histograms of the values of the  $CP$  phases  $\phi_{1,2,\mu,t,b}$  after applying the current (blue histogram, model set C) and future (green histogram, model set D) constraints on the observables in Table III. In showing the expected future constraints, we once again emphasize our assumption that experimental measurements will obtain the SM predictions given in Table III. These figures demonstrate the high sensitivity of future flavor experiments to the phases  $\phi_1$ ,  $\phi_2$ ,  $\phi_\mu$ , and  $\phi_t$ . Null results from future experiments would require  $\phi_2$  and  $\phi_\mu$  to be small,  $\mathcal{O}(10^{-2})$  or less, while weaker limits of  $\mathcal{O}(10^{-1})$  would be placed on  $\phi_1$  and  $\phi_t$ . Interestingly,  $\mathcal{O}(1)$  values of  $\phi_b$  would remain essentially unconstrained. We note that  $\phi_\tau$  (not shown) also remains unconstrained.

Figure 1 displays a two-dimensional density histogram of the phases  $\phi_2$  and  $\phi_\mu$  for the models that pass current constraints (model set C) and illustrates interesting correlations. Note that there is a region with  $\phi_2 \approx \phi_\mu$  where  $\mathcal{O}(1)$  values of both phases are allowed. This corresponds to the case where the most significant effective phase contributing to the EDMs is effectively zero, due to a cancellation among gaugino exchange diagrams [69]. Due to this cancellation, models with large and nearly equal phases  $\phi_2$  and  $\phi_\mu$  survive the EDM bounds. These models are, however, tuned in the sense that they are delicately sensitive to the degree of cancellation between these phases.

The observables that are most sensitive to  $CP$ -violating effects are the electron and neutron EDMs, as well as  $\sin 2\beta$  and  $\epsilon_K$ . The upper four panels of Fig. 2 show histograms of these quantities, demonstrating the potential of individual experiments to constrain these observables or detect NP arising from SUSY. In each panel, the upper histogram corresponds to models that have passed all the current constraints (blue, model set C), while the lower histogram (green) is obtained by applying anticipated future constraints from all observables except for the one under study. The expected future limit on the EDMs is represented by

the vertical lines. Here, we see the well-known feature that future EDM constraints will be very important in probing supersymmetric  $CP$  phases. We note, however, that the expected future measurements for  $\sin 2\beta$  and  $\epsilon_K$  lie outside the ranges shown in the histograms, indicating that improved measurements of these quantities will not further constrain these models. We observe that there is a large correlation between  $\sin 2\beta$  and the EDMs, as the models passing future constraints (dominated by EDM limits) cluster around the SM expectations for  $\sin 2\beta$ .

If future EDM experiments continue to obtain null results, a non-SM measurement of  $\sin 2\beta$  would thus pose an intriguing challenge to the  $CP$ -violating pMSSM. On the other hand, we see that  $\epsilon_K$  is not particularly sensitive to the gaugino phases and is therefore poorly correlated with the other  $CP$ -violating observables. A relatively large deviation from the SM in  $\epsilon_K$  would still be possible, even if future EDM searches are null. The lower two panels of Fig. 2 display two-dimensional histograms of these observables for models in agreement with the current experimental constraints (model set C). The lines in Fig. 2(e) correspond to the anticipated future limits listed in Table III. These figures serve to further illustrate the correlations among  $CP$ -violating observables. We see that the electron and neutron EDMs are strongly aligned as expected, while there is no correlation between  $\sin 2\beta$  and  $\epsilon_K$ , due to the latter's lack of sensitivity to the gaugino phases.

To further explore the constraints placed on the phases, Fig. 3 contains two-dimensional histograms showing the neutrino and electrons EDMs paired with  $\phi_1$ ,  $\phi_2$ , or  $\phi_\mu$  for models that are allowed by current constraints (model set C). The anticipated future EDM search reach corresponds to the horizontal line. The electron EDM provides a particularly strong constraint on large values of all three phases. Most models with phases larger than  $\sim 10^{-1}$  are already excluded, and the parameter space will be further explored by an order of magnitude in the values of the phases to roughly  $10^{-2}$ . However, some room remains for rather large values of the phases due to possible cancellations of the contributions arising from  $\phi_\mu$  and  $\phi_2$  as described above.

Low-energy observables that are sensitive to the  $A$ -term phases  $\phi_t$ ,  $\phi_b$ , and  $\phi_\tau$  must involve flavor-violating couplings. The most sensitive such observables that are incorporated in `SUSY_FLAVOR` are  $\sin 2\beta$  and  $\epsilon_K$ . The dependence on  $\phi_b$  and  $\phi_\tau$  in these observables is extremely weak;  $\phi_b$  contributions are typically suppressed by  $m_b$  (except possibly at large  $\tan\beta$ ), while  $\phi_\tau$  would contribute only to  $\tau$  flavor-violating processes or poorly measured observables such as the  $\tau$  EDM. The impact of  $\phi_t$  on the electron and neutron EDMs, as well as on  $\sin 2\beta$  and  $\epsilon_K$ , is shown in Fig. 4. Unlike the structure illustrated in Fig. 3, we see that there is no correlation between most of these quantities and the phase  $\phi_t$ . We note that a mild constraint

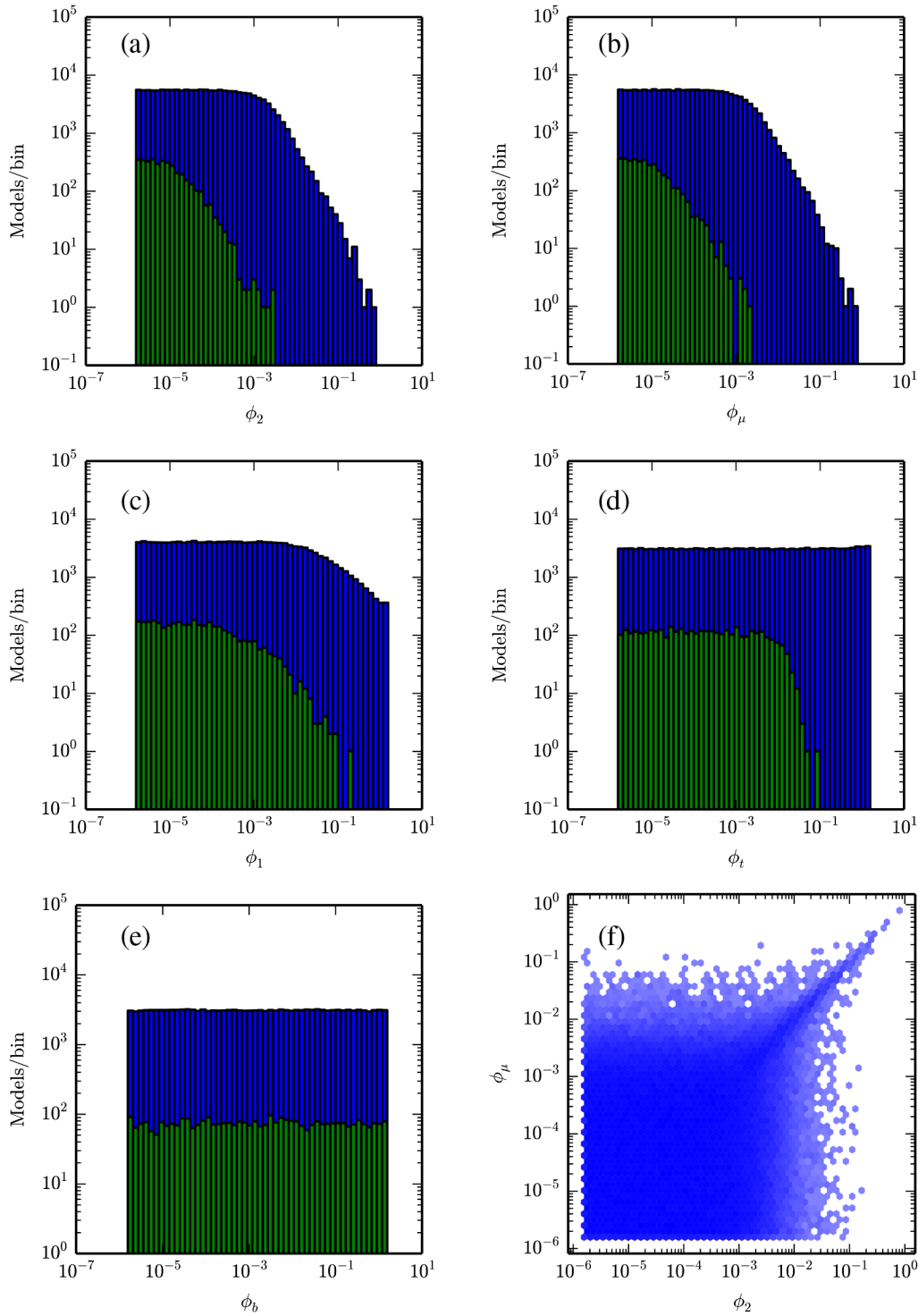


FIG. 1. (a)–(e): Distributions of the  $CP$ -violating phases  $\phi_{1,2,\mu,t,b}$  added to the pMSSM in model sets C (blue) and D (green). (f): Model densities of values for the phases  $\phi_2$  and  $\phi_\mu$  in model set C. The shading ranges from light blue to dark blue with the darkness being logarithmic in the number of models in the bin. White bins contain no models. The model sets are defined in Table II.

on models with large  $\phi_t$  is possible from the neutron EDM; however, improving the precision on  $\sin 2\beta$  and  $\epsilon_K$  does not bound these phases.

Next, we consider the correlation between low-energy observables and direct LHC searches for supersymmetry in

order to determine the degree of complementarity between the two approaches for probing supersymmetry. To do so, we consider models that are expected [27] to evade Jets + MET and stop-squark searches at the LHC with  $3000 \text{ fb}^{-1}$  of integrated luminosity (extracted from model sets C and

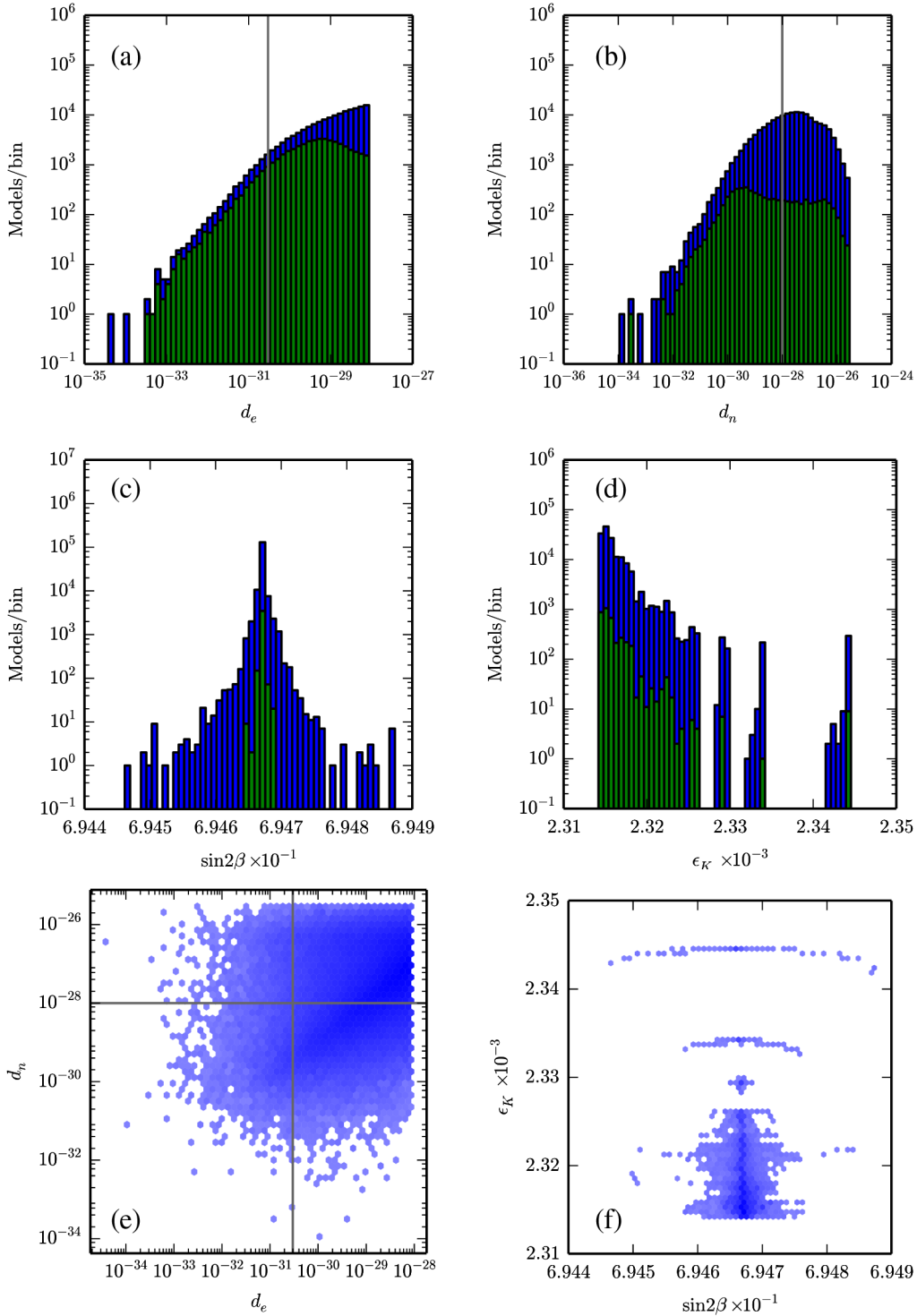


FIG. 2. (a)–(d): Expected constraints from future low-energy experiments on the pMSSM models with  $CP$  violation. In each panel, the top histogram shows models after applying current constraints (blue, model set C), while the bottom histogram (green) represents the remaining models after applying all future constraints except for the observable under study. This illustrates the exclusive ability of that observable to probe the model parameter space. Where possible, the anticipated future limit on the observable is indicated by a vertical or horizontal line. (e)–(f): Model densities for the observables in model set C. The shading is as in Fig. 1(f).

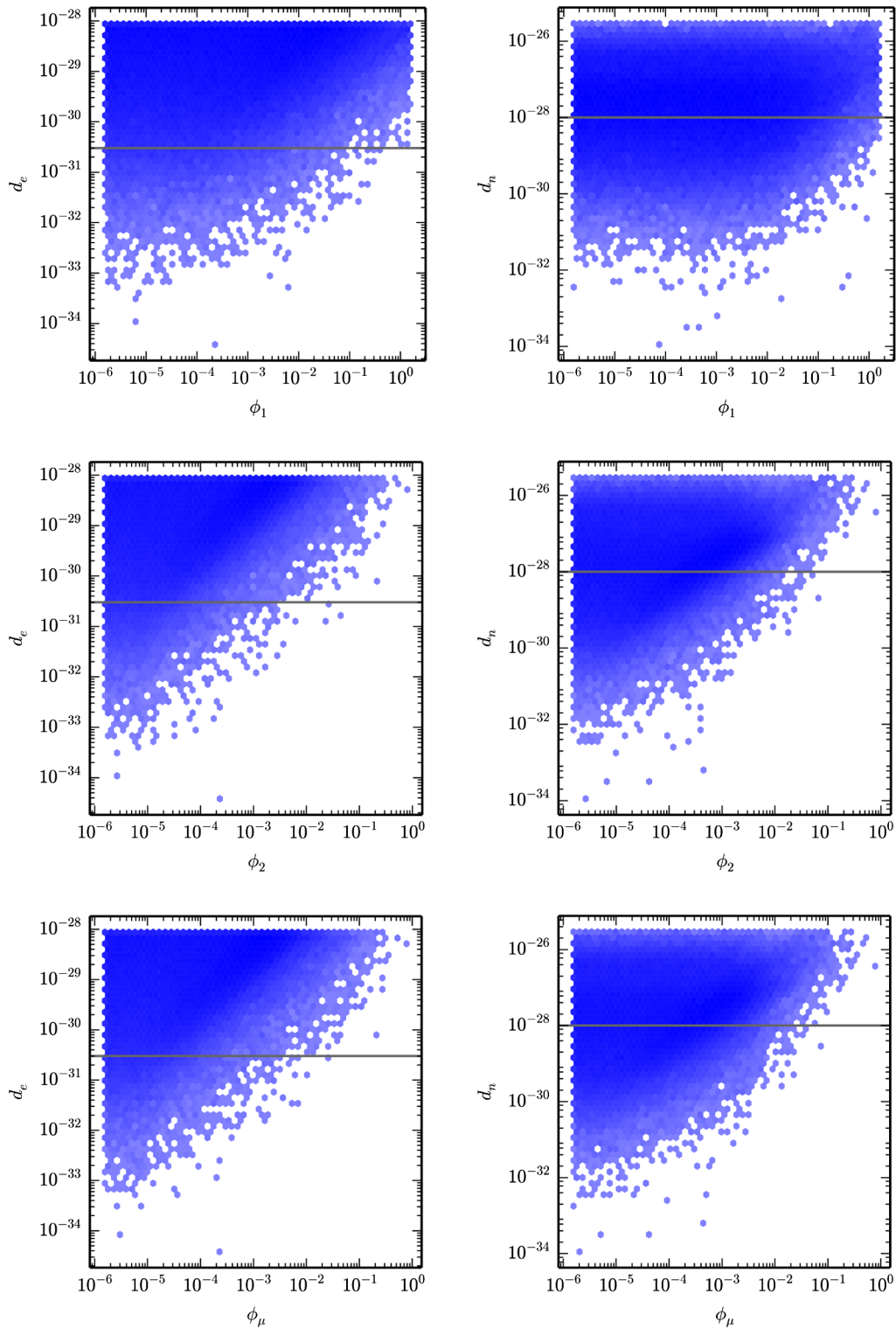


FIG. 3. Model densities for the electron and neutron EDMs as a function of the phases  $\phi_1$ ,  $\phi_2$ , and  $\phi_\mu$  in model set C. The shading is as in Fig. 1(f). The lines indicate the future expected EDM reaches.

D). Figure 5 shows a comparison of the impact of low-energy experiments to that of direct LHC searches in exploring the pMSSM models with  $CP$  phases. In all cases, we see that the shape of the distribution remains

essentially unchanged, and only the number of viable models is affected by the LHC searches. Hence, the ability of the current and future measurements of low-energy observables to constrain models is observed to be

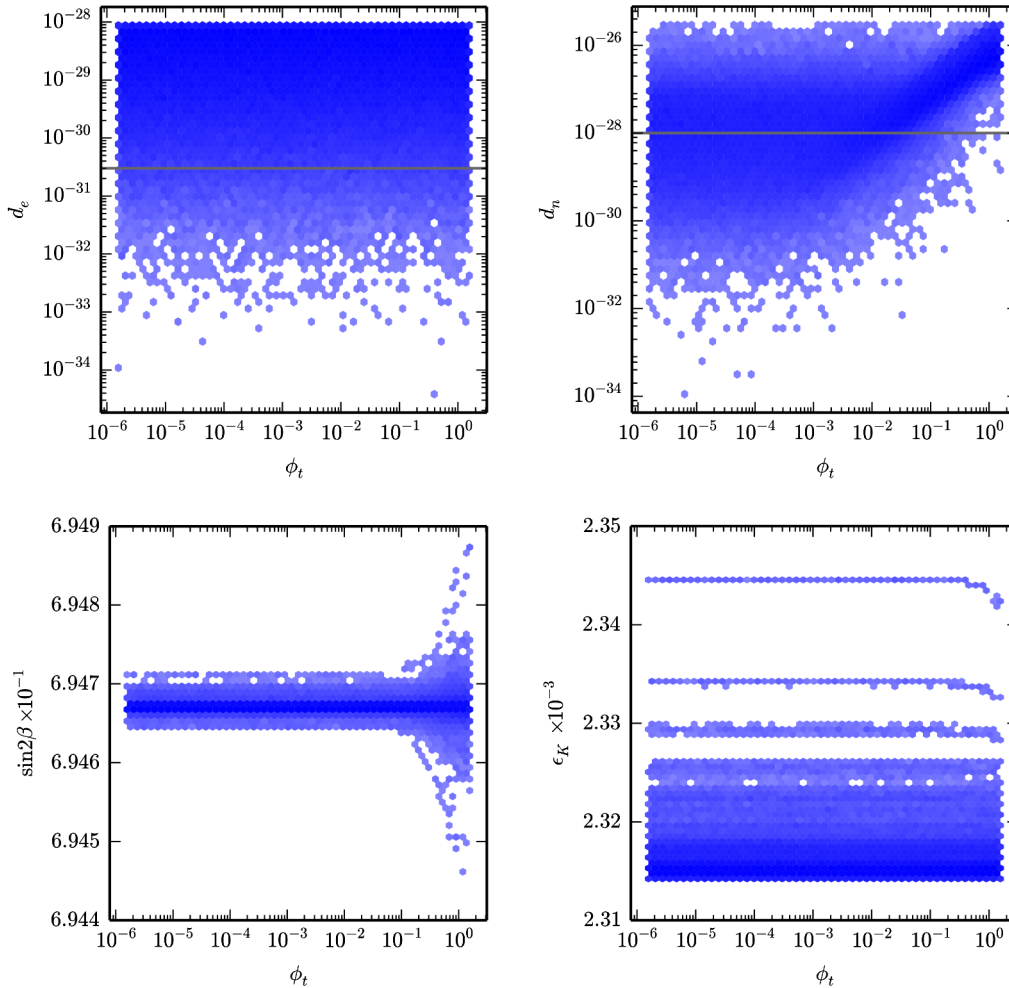


FIG. 4. Model densities for the electron and neutron EDMs,  $\sin 2\beta$ , and  $\epsilon_K$  as a function of the phase  $\phi_t$  in model set C. The shading is as in Fig. 1(f). The horizontal lines in the top panels indicate expected future EDM limits. The expected future constraints on  $\sin 2\beta$  and  $\epsilon_K$  lie outside the ranges of the lower panels.

independent of the discovery reach of the LHC. These results indicate a high degree of complementarity between the low-energy  $CP$  violation experiments and the direct SUSY searches at the LHC as probes of the MSSM.

Although the main thrust of this work is to study  $CP$ -violating observables, flavor-changing  $CP$ -conserving observables, as well as the anomalous magnetic moment of the muon, are also sensitive to the presence of  $CP$ -violating phases. We therefore next examine the most sensitive flavor-violating,  $CP$ -conserving observables to study their sensitivity to the pMSSM phases. In Figs. 6 and 7, we compare the predicted rates of various processes in the original  $CP$ -conserving pMSSM (model set A on the  $x$  axis) with their  $CP$ -violating counterparts (model set C on the  $y$  axis). While we see a strong correlation between the two model sets in the  $CP$ -conserving processes, it is clear that the presence of phases leads to some interesting effects.

In particular,  $\text{Br}(B_{s,d} \rightarrow \mu^+\mu^-)$  and  $\text{Br}(B \rightarrow X_s\gamma)$  both experience nontrivial contributions from supersymmetric

$CP$  phases, and future experiments should have a significant sensitivity to these contributions. It is particularly noteworthy that, while some of the  $CP$ -conserving pMSSM models are expected to be probed by future measurements of  $\text{Br}(B \rightarrow X_s\gamma)$  and  $\text{Br}(B_s \rightarrow \mu^+\mu^-)$ , introducing  $CP$ -violating phases has the potential to bring predictions for these processes *back into agreement* with the SM rates.

In particular, the ratio of  $\text{Br}(B_s \rightarrow \mu^+\mu^-)$  in the MSSM to that in the SM can be written to a very good approximation in the following way,

$$\frac{\text{Br}(B_s \rightarrow \mu^+\mu^-)|_{\text{MSSM}}}{\text{Br}(B_s \rightarrow \mu^+\mu^-)|_{\text{SM}}} = |X|^2 + |1 + X|^2, \quad (3)$$

where  $X$  is the new contribution from the supersymmetric partners. Writing  $X$  as  $X = \pm x e^{i\theta}$ , Eq. (3) reduces to (here  $x$  is taken to be positive by convention and, barring large cancellation, must satisfy  $x \ll 1$  to be consistent with experiment)

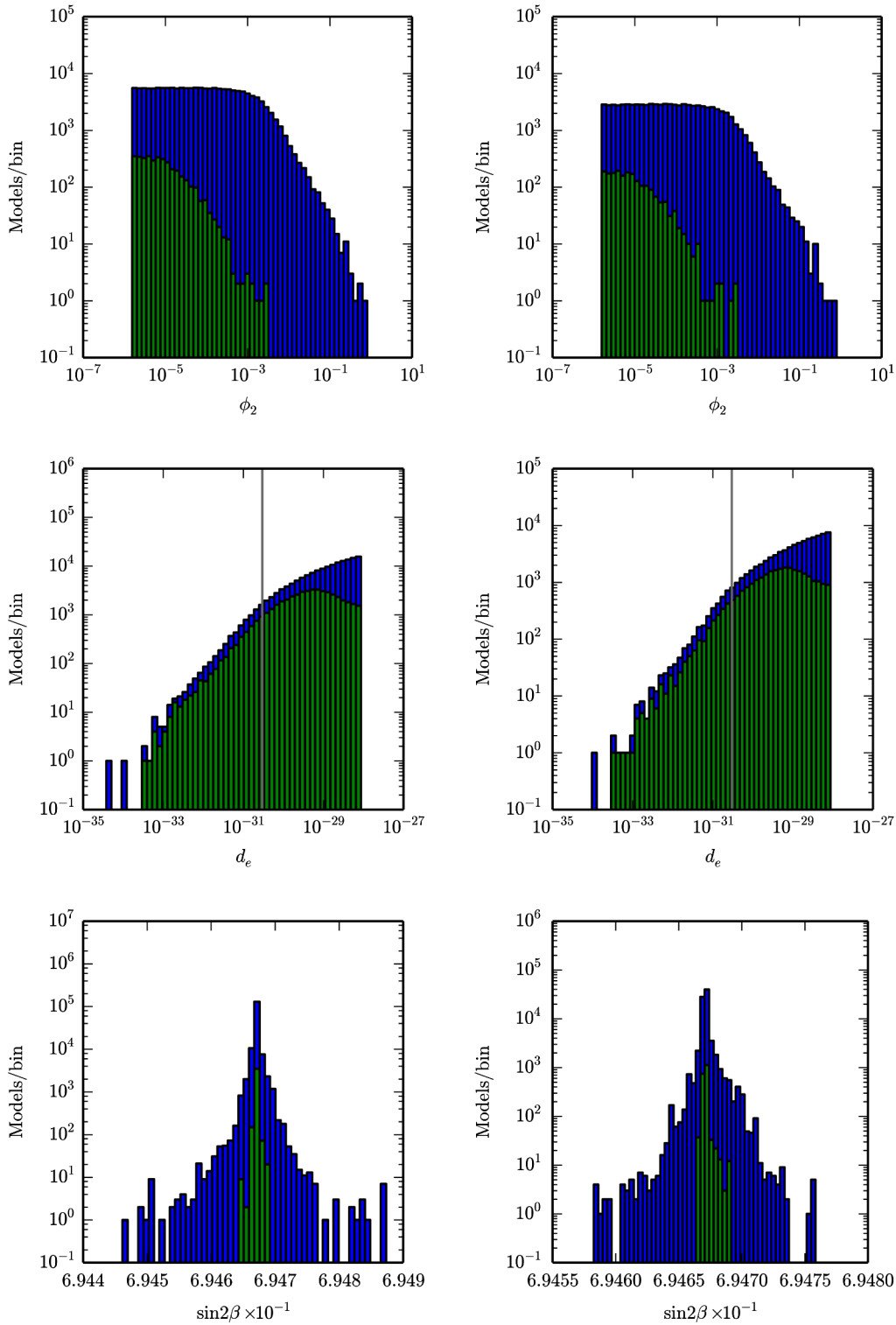


FIG. 5. Complementarity between the low-energy experiments and the direct SUSY searches at the LHC. The left panels are identical to Figs. 1(a), 2(a), and 2(c), respectively. The right panels are the corresponding figures including only those models that are expected to evade the leading 14 TeV LHC direct SUSY searches with 3000 fb<sup>-1</sup> of integrated luminosity. Note the difference in the scales of the vertical axes between the left and right panels.

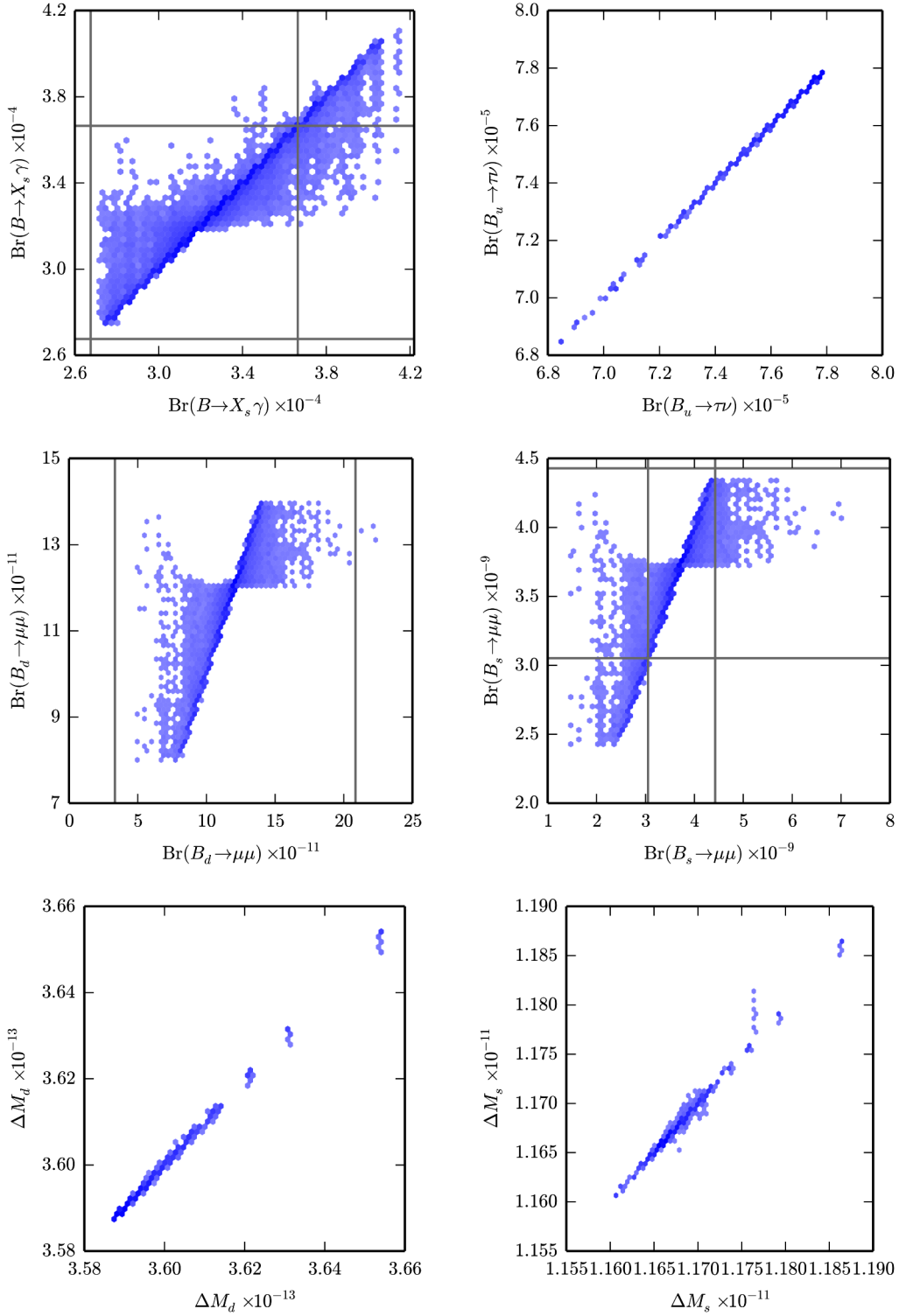


FIG. 6. Comparison of several flavor-changing,  $CP$ -conserving  $B$  physics observables in the original pMSSM models without  $CP$  violation (model set A on the horizontal axes) and the corresponding models with randomly selected phases (model set C on the vertical axes). The lines indicate future expected measurements on the various observables. The shading is as in Fig. 1(f).

$$\frac{\text{Br}(B_s \rightarrow \mu^+ \mu^-)|_{\text{MSSM}}}{\text{Br}(B_s \rightarrow \mu^+ \mu^-)|_{\text{SM}}} = x^2 + |1 \pm x e^{i\theta}|^2 \quad (4)$$

$$= 1 \pm 2x \cos \theta + 2x^2. \quad (5)$$

Clearly, for a given value of  $x$ , the above ratio maximally deviates from unity at  $\theta = 0$ , and any finite nonzero value of the phase  $\theta$  will always push it closer to the SM. Note that the above argument is strictly correct only in the case

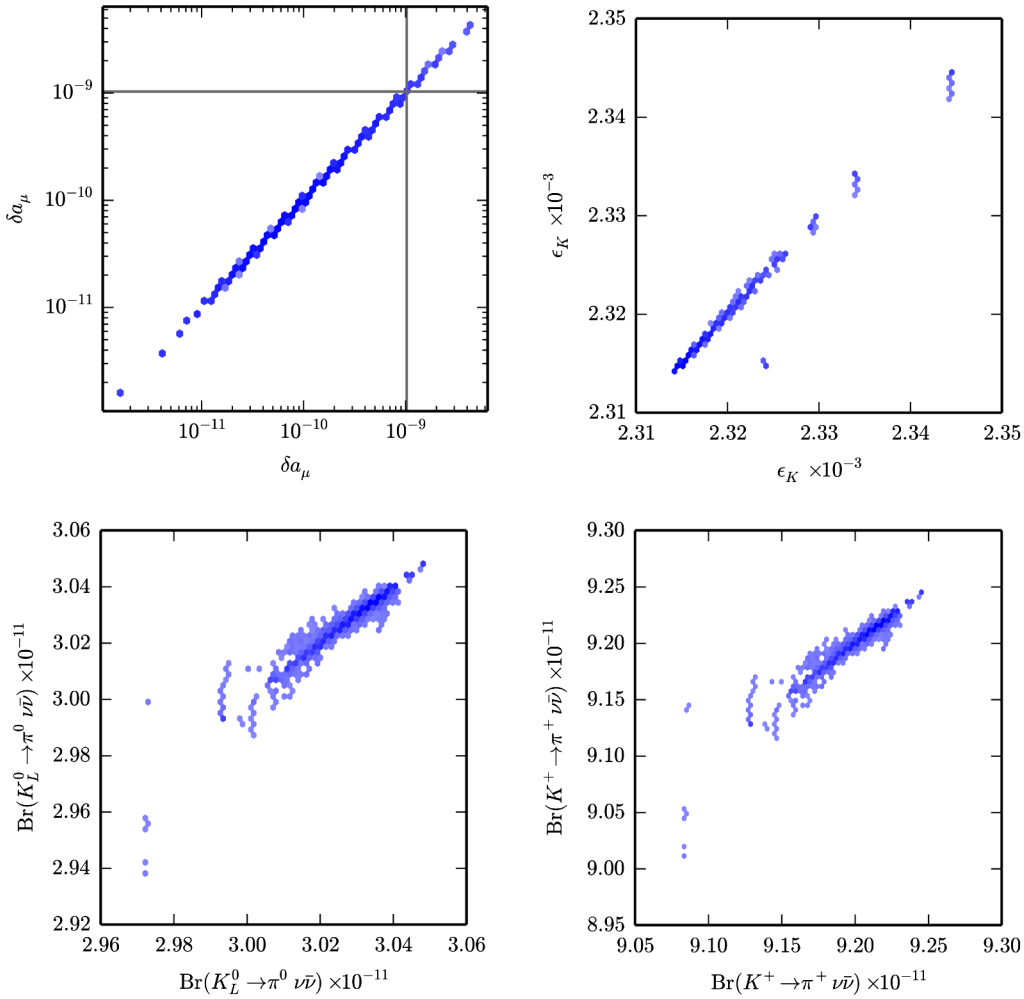


FIG. 7. Same as Fig. 6, but for the anomalous magnetic moment of the muon, as well as rare Kaon processes.

when the NP amplitude has a single contribution. However, even in the presence of multiple contributions, if one of them is the dominant term [which is indeed the case here because the Higgsino contribution dominates in most of the parameter space where the constraint from  $\text{Br}(B_s \rightarrow \mu^+ \mu^-)$  is important] or there are no large cancellations among the various terms, the above argument still holds.

We also see some cases where the addition of  $CP$  phases creates a signal in one of these flavor-changing processes that would be detectable by future experiments; this effect, however, is found to be far less common. Note that the rare Kaon processes generally tend to not exhibit these effects and thus are much less sensitive to the presence of  $CP$  phases.

We also consider the pMSSM contributions to the anomalous magnetic moment of the muon,  $\delta a_\mu$ . As is well known, there is presently a claim [47] of an observation of a  $> 3\sigma$  deviation in this observable from the current SM prediction. If this deviation were to be confirmed by future experimental results, it would impose a particularly strong constraint on the models considered in this work. Since there remains some controversy surrounding the theoretical

calculation, and the measurement itself has yet to be independently confirmed, we have not imposed cuts on  $\delta a_\mu$  in applying current low-energy constraints to our models (model set C in particular). However, we note that if the current experimental result for  $\delta a_\mu$  were to be applied at the  $2\sigma$  level, only 952 models in model set C would survive. In addition, we have projected the impact of upcoming low-energy measurements, assuming that the SM value of  $\delta a_\mu$  will be confirmed in the future (model set D). It is also interesting to examine the power of a future  $\delta a_\mu$  measurement which is in agreement with the existing experimental result, e.g., the same central value but with the smaller error bars that may arise from the Muon  $g - 2$  Collaboration. If the current measurement of  $\delta a_\mu$  persists but with the errors reduced as projected by the Muon  $g - 2$  Collaboration, then none of the models in model set D would remain viable. On the other hand, if the same future result is consistent with the SM, then the measurement of  $\delta a_\mu$  would not provide any exclusionary power beyond the other low-energy measurements. In other words, all models that would remain viable from other future low-energy flavor and  $CP$ -violation experiments are consistent with the

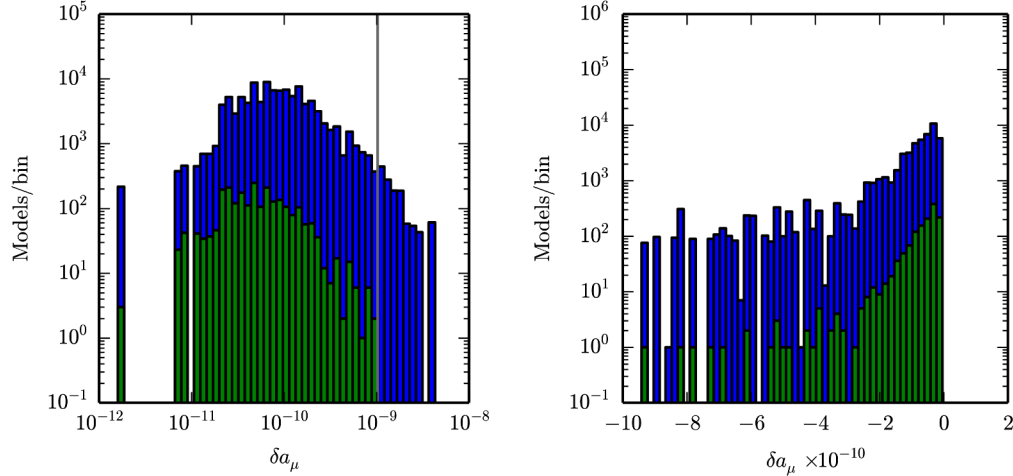


FIG. 8. Predicted distributions of  $\delta a_\mu$  for positive (left) and negative (right) values of this observable. Due to the large range of possible values for  $\delta a_\mu$  in these models, the positive values are shown on a log scale, while negative values are displayed on a linear scale. Models surviving current (model set C) and future (model set D) low-energy constraints are shown in blue and green, respectively, assuming the future results agree with the SM, i.e.,  $\delta a_\mu = 0$ . The vertical line indicates the expected bound on  $\delta a_\mu$  under this assumption and shows that this measurement would not exclude models beyond the search reach of other future low-energy processes.

SM prediction of  $\delta a_\mu$  within the future anticipated sensitivity of the Muon  $g - 2$  experiment. These results are shown explicitly in Fig. 8, displaying the distribution of  $\delta a_\mu$  in the  $CP$ -violating pMSSM model sets consistent with the current and expected future low-energy constraints. Note that the current  $2\sigma$  lower limit on  $\delta a_\mu$  is  $11.6 \times 10^{-10}$  since it differs from zero by over  $3\sigma$ .

In Table V, we compile the fraction of models from set B ( $CP$  violating) that are projected to remain viable after the most sensitive future low-energy measurements are completed, as well as the fraction of models from set A ( $CP$  conserving) for which at least one correlated model in set B is projected to satisfy the constraints. Clearly, the neutron and electron EDMs provide the best sensitivity (strongest constraints or larger discovery reach) to the presence of

TABLE V. The fraction of models in set B ( $CP$  violating) that are projected to remain viable after the most sensitive future low-energy measurements are performed, as well as the fraction of models in set A ( $CP$  conserving) for which at least one correlated model in set B is projected to satisfy constraints. The  $(g - 2)_\mu$  entries assume that the currently observed central value continues to hold while the corresponding uncertainties shrink as projected in Ref. [1]. The  $(g - 2)_\mu$  constraint is not included in the “All future” row.

Observable	Fraction of B models	Fraction of A models
$d_e$	0.00645	0.746
$d_n$	0.0539	0.764
$\text{Br}(B^+ \rightarrow X_s \gamma)$	0.144	0.877
$\text{Br}(B_s \rightarrow \mu^+ \mu^-)$	0.148	0.888
$(g - 2)_\mu$	0.000366	0.009
All future	0.00371	0.587

phases in the  $CP$ -violating pMSSM, while other observables also provide good sensitivity to these NP effects. For the case of  $(g - 2)_\mu$ , we assume that future experiment will uphold the current central value. In addition, we show the fraction of models that survive after the combination of all future low-energy measurements [neglecting  $(g - 2)_\mu$ ] is performed. This corresponds to only  $\sim 0.4\%$  of the original  $10^6$  models generated, demonstrating the power of low-energy observables in searching for supersymmetric  $CP$ -violating effects.

#### IV. DISCUSSION AND CONCLUSIONS

This study explored the complementarity of indirect low-energy probes of the MSSM with those arising from direct SUSY searches at the LHC. The broad suite of future low-energy experiments examined here include flavor-violating decays of the  $K$  and  $B_{d,s}$  mesons—with and without  $CP$ -violating observables, meson mixing, the  $g - 2$  of the muon, and EDMs. To perform this investigation we employed a previously examined set of  $10^3$   $CP$ -conserving pMSSM models (described by specific values of the 19 pMSSM parameters) that satisfy existing experimental constraints, including the value of the observed Higgs boson mass and the direct LHC SUSY searches. For each of these thousand models, we generated  $10^3$  sets of  $CP$ -violating phases, corresponding to those associated with the parameters  $M_{1,2}, \mu$ , and  $A_{t,b,\tau}$ , thus yielding a total of  $10^6$  models that we then employ in our study. This large set of models was then divided into various useful subsets depending upon how a given model is expected to respond to the anticipated 13 TeV LHC direct SUSY searches, as well as both the present and future set of flavor- and

CP-violating measurements. The sensitivity to the different types of experiments can then be contrasted and compared with these various subsets.

The main result from this study is that we have shown in a quantitative manner that direct SUSY searches at the LHC and measurement of the low-energy observables considered here are almost orthogonal in their sensitivity and probe the CP-violating pMSSM parameter space in completely different ways. In particular, we find that the low-energy measurements can probe pMSSM models that lie outside of the range of the 13 TeV LHC, even when the CP-violating phases take on modest values. However, we also find regions of parameter space where large phases remain allowed due to a cancellation between the contributions to CP-violating observables, particularly the electron and neutron EDMs. Furthermore, we have also found that the added flexibility derived from the inclusion of the phases can bring the pMSSM predictions closer to the observed experimental results, and Standard Model expectations, for rare processes such as  $B_s \rightarrow \mu^+ \mu^-$  which are seen to be highly restrictive in the absence of such phases.

Of course the true impact of future low-energy observables will be highly correlated with the actual measured values; this is most obvious in the cases of the electron and neutron EDMs and the  $g - 2$  of the muon. In the case of the EDMs, a null measurement will severely constrain the CP-violating pMSSM parameter space, especially if the

anticipated sensitivity of future measurements is reached. On the other hand, a measurement of  $g - 2$  with the presently observed central value, but with significantly reduced experimental (and theoretical) errors, would be extremely constraining on this parameter space independently of what is found by the direct SUSY searches at the LHC. However, if the SM prediction for  $g - 2$  is obtained with smaller errors, then the impact on the pMSSM parameter space will turn out to be rather modest.

Although constrained by existing searches, the viable SUSY parameter space still remains quite large. Hopefully, multiple signals for supersymmetry will be discovered by a diverse set of experiments during the next few years.

## ACKNOWLEDGMENTS

We are grateful for the help of Janusz Rosiek for updating the `SUSY_FLAVOR` code. This work was supported by the Department of Energy, Contracts No. DE-AC02-06CH11357, No. DE-AC02-76SF00515, and No. DE-FG02-12ER41811. D. G. has received support from the European Research Council (ERC) under the European Union's Seventh Framework Programme (FP/2007-2013)/ERC Grant No. 279972. D. G. would also like to gratefully acknowledge the hospitality and support by the SLAC Theory Group where part of this work was done.

- 
- [1] J. Hewett *et al.*, Fundamental Physics at the Intensity Frontier, [arXiv:1205.2671](https://arxiv.org/abs/1205.2671).
  - [2] J. Hewett *et al.*, Planning the future of U.S. particle physics (Snowmass 2013): Chapter 2: intensity frontier, [arXiv:1401.6077](https://arxiv.org/abs/1401.6077).
  - [3] M. Antonelli *et al.*, Flavor physics in the quark sector, *Phys. Rep.* **494**, 197 (2010).
  - [4] J. Hewett, T. Takeuchi, and S. D. Thomas, Indirect Probes of New Physics, [arXiv:hep-ph/9603391](https://arxiv.org/abs/hep-ph/9603391).
  - [5] J. Charles J. Charles, A. Höcker, H. Lacker, S. Laplace, F. R. Diberder, J. Malclés, J. Ocariz, M. Pivk, and L. Roos (CKMfitter Group Collaboration), CP violation and the CKM matrix: Assessing the impact of the asymmetric B factories, *Eur. Phys. J. C* **41**, 1 (2005). Updated results and plots available at <http://ckmfitter.in2p3.fr>.
  - [6] M. Ciuchini V. Lubicz, G. D'Agostini, E. Franco, G. Martinelli, F. Parodi, P. Roudeau, and A. Stocchi, 2000 CKM triangle analysis: A critical review with updated experimental inputs and theoretical parameters, *J. High Energy Phys.* **07** (2001) 013.
  - [7] O. Buchmueller *et al.*, Frequentist analysis of the parameter space of minimal supergravity, *Eur. Phys. J. C* **71**, 1583 (2011).
  - [8] B. Bhattacharjee, A. Dighe, D. Ghosh, and S. Raychaudhuri, Do new data on  $B^+ \rightarrow \tau^+ \nu_\tau$  decays point to an early discovery of supersymmetry at the LHC?, *Phys. Rev. D* **83**, 094026 (2011).
  - [9] D. Ghosh, M. Guchait, S. Raychaudhuri, and D. Sengupta, How constrained is the cMSSM?, *Phys. Rev. D* **86**, 055007 (2012).
  - [10] A. Arbey, M. Battaglia, F. Mahmoudi, and D. Martinez Santos, Supersymmetry confronts  $B_s \rightarrow \mu^+ \mu^-$ : Present and future status, *Phys. Rev. D* **87**, 035026 (2013).
  - [11] A. Dighe, D. Ghosh, K. M. Patel, and S. Raychaudhuri, Testing times for supersymmetry: Looking under the lamp post, *Int. J. Mod. Phys. A* **28**, 1350134 (2013).
  - [12] J. R. Ellis and D. V. Nanopoulos, Flavor changing neutral interactions in broken supersymmetric theories, *Phys. Lett.* **110B**, 44 (1982).
  - [13] D. Chang, W.-Y. Keung, and A. Pilaftsis, New Two Loop Contribution to Electric Dipole Moment in Supersymmetric Theories, *Phys. Rev. Lett.* **82**, 900 (1999).
  - [14] S. P. Martin, A supersymmetry primer, *Adv. Ser. Dir. High Energy Phys.* **21**, 1 (2010).
  - [15] G. Isidori, Y. Nir, and G. Perez, Flavor physics constraints for physics beyond the Standard Model, *Annu. Rev. Nucl. Part. Sci.* **60**, 355 (2010).

- [16] W. Altmannshofer, R. Harnik, and J. Zupan, Low energy probes of PeV scale sfermions, *J. High Energy Phys.* **11** (2013) 202.
- [17] G. Giudice and R. Rattazzi, Theories with gauge mediated supersymmetry breaking, *Phys. Rep.* **322**, 419 (1999).
- [18] G. F. Giudice, M. A. Luty, H. Murayama, and R. Rattazzi, Gaugino mass without singlets, *J. High Energy Phys.* **12** (1998) 027.
- [19] L. Randall and R. Sundrum, Out of this world supersymmetry breaking, *Nucl. Phys.* **B557**, 79 (1999).
- [20] A. Pomarol and R. Rattazzi, Sparticle masses from the superconformal anomaly, *J. High Energy Phys.* **05** (1999) 013.
- [21] A. Djouadi *et al.* (MSSM Working Group Collaboration), The minimal supersymmetric standard model: Group summary report, [arXiv:hep-ph/9901246](https://arxiv.org/abs/hep-ph/9901246).
- [22] C. F. Berger, J. S. Gainer, J. L. Hewett, and T. G. Rizzo, Supersymmetry without prejudice, *J. High Energy Phys.* **02** (2009) 023.
- [23] M. Carena, J. R. Ellis, A. Pilaftsis, and C. Wagner, Higgs boson pole masses in the MSSM with explicit  $CP$  violation, *Nucl. Phys.* **B625**, 345 (2002).
- [24] M. Cahill-Rowley, R. Cotta, A. Drlica-Wagner, S. Funk, J. L. Hewett, A. Ismail, T. G. Rizzo, and M. Wood, Complementarity of dark matter searches in the phenomenological MSSM, *Phys. Rev. D* **91**, 055011 (2015).
- [25] J. Berger *et al.*, The  $CP$ -violating pMSSM at the Intensity Frontier, [arXiv:1309.7653](https://arxiv.org/abs/1309.7653).
- [26] M. W. Cahill-Rowley, J. L. Hewett, S. Hoeche, A. Ismail, and T. G. Rizzo, The new look pMSSM with neutralino and gravitino LSPs, *Eur. Phys. J. C* **72**, 2156 (2012).
- [27] M. Cahill-Rowley, J. Hewett, A. Ismail, and T. Rizzo, Lessons and prospects from the pMSSM after LHC Run I, *Phys. Rev. D* **91**, 055002 (2015).
- [28] S. Heinemeyer, Higgs physics in the SM and the MSSM, SUSY 2014: The 22nd International Conference on Supersymmetry and Unification of Fundamental Interactions, Manchester, England, 2014 (unpublished), <http://indico.hep.manchester.ac.uk/getFile.py/access?contribId=64&resId=0&materialId=slides&confId=4221>.
- [29] A. Crivellin, J. Rosiek, P. H. Chankowski, A. Dedes, S. Jäger, and P. Tanedo, SUSY\_FLAVOR v2: A Computational tool for FCNC and  $CP$ -violating processes in the MSSM, *Comput. Phys. Commun.* **184**, 1004 (2013).
- [30] A. J. Buras, T. Ewerth, S. Jager, and J. Rosiek,  $K^+ \rightarrow \pi^+ \nu \bar{\nu}$  and  $K_L \rightarrow \pi^0 \nu \bar{\nu}$  decays in the general MSSM, *Nucl. Phys.* **B714**, 103 (2005).
- [31] A. Dedes, J. Rosiek, and P. Tanedo, Complete one-loop MSSM predictions for  $B \rightarrow \ell^+ \ell^-$  at the Tevatron and LHC, *Phys. Rev. D* **79**, 055006 (2009).
- [32] M. Pospelov and I. Khriplovich, Electric dipole moment of the W boson and the electron in the Kobayashi-Maskawa model, *Sov. J. Nucl. Phys.* **53**, 638 (1991).
- [33] M. J. Booth, The electric dipole moment of the W and electron in the standard model, [arXiv:hep-ph/9301293](https://arxiv.org/abs/hep-ph/9301293).
- [34] J. Baron *et al.* (ACME Collaboration), Order of magnitude smaller limit on the electric dipole moment of the electron, *Science* **343**, 269 (2014).
- [35] A. C. Vutha *et al.*, Search for the electric dipole moment of the electron with thorium monoxide, *J. Phys. B* **43**, 074007 (2010).
- [36] B. Wundt, C. Munger, and U. Jentschura, Quantum dynamics in atomic-fountain experiments for measuring the electric dipole moment of the electron with improved sensitivity, *Phys. Rev. X* **2**, 041009 (2012).
- [37] D. Bowser-Chao, D. Chang, and W.-Y. Keung, Electron Electric Dipole Moment from  $CP$  Violation in the Charged Higgs Sector, *Phys. Rev. Lett.* **79**, 1988 (1997).
- [38] G. Bennett *et al.* (Muon (g-2) Collaboration), An improved limit on the muon electric dipole moment, *Phys. Rev. D* **80**, 052008 (2009).
- [39] F. J. M. Farley, K. Jungmann, J. P. Miller, W. M. Morse, Y. F. Orlov, B. L. Roberts, Y. K. Semertzidis, A. Silenko, and E. J. Stephenson, A New Method of Measuring Electric Dipole Moments in Storage Rings, *Phys. Rev. Lett.* **93**, 052001 (2004).
- [40] E. Shabalin, The electric dipole moment of the neutron in a gauge theory, *Sov. Phys. Usp.* **26**, 297 (1983).
- [41] B. H. McKellar, S. Choudhury, X. G. He, and S. Pakvasa, The neutron electric dipole moment in the standard KM model, *Phys. Lett. B* **197**, 556 (1987).
- [42] C. Baker *et al.*, An Improved Experimental Limit on the Electric Dipole Moment of the Neutron, *Phys. Rev. Lett.* **97**, 131801 (2006).
- [43] I. Altarev *et al.*, Towards a new measurement of the neutron electric dipole moment, *Nucl. Instrum. Methods Phys. Res., Sect. A* **611**, 133 (2009).
- [44] T. Aoyama, M. Hayakawa, T. Kinoshita, and M. Nio, Revised value of the eighth-order QED contribution to the anomalous magnetic moment of the electron, *Phys. Rev. D* **77**, 053012 (2008).
- [45] D. Hanneke, S. Fogwell, and G. Gabrielse, New Measurement of the Electron Magnetic Moment and the Fine Structure Constant, *Phys. Rev. Lett.* **100**, 120801 (2008).
- [46] T. Blum *et al.*, The Muon (g-2) Theory Value: Present and Future, [arXiv:1311.2198](https://arxiv.org/abs/1311.2198).
- [47] G. Bennett *et al.* (Muon G-2 Collaboration), Final report of the muon E821 anomalous magnetic moment measurement at BNL, *Phys. Rev. D* **73**, 072003 (2006).
- [48] F. Mescia and C. Smith, Improved estimates of rare K decay matrix-elements from  $K_{l3}$  decays, *Phys. Rev. D* **76**, 034017 (2007).
- [49] J. Ahn *et al.* (E391a Collaboration), Experimental study of the decay  $K_L^0 \rightarrow \pi^0 \nu \bar{\nu}$ , *Phys. Rev. D* **81**, 072004 (2010).
- [50] J. Beringer *et al.* (KOTO Collaboration), Proposal for a  $K_L \rightarrow \pi \nu \nu$  Experiment at J-PARC, J-PARC Experimental Proposal (2006), <http://koto.kek.jp/pub/p14.pdf>.
- [51] A. Artamonov *et al.* (E949 Collaboration), New Measurement of the  $K^+ \rightarrow \pi^+ \nu \bar{\nu}$  Branching Ratio, *Phys. Rev. Lett.* **101**, 191802 (2008).
- [52] E. Worcester (ORKA Collaboration), ORKA, the golden kaon experiment: Precision measurement of  $K^+ \rightarrow \pi^+ \nu \bar{\nu}$  and other rare processes, *Proc. Sci.*, KAON13 (2013) 035.
- [53] M. Misiak *et al.*, Estimate of  $BR(B \rightarrow X_s \gamma)$  at  $\mathcal{O}(\alpha_s^2)$ , *Phys. Rev. Lett.* **98**, 022002 (2007).
- [54] Y. Amhis *et al.* (Heavy Flavor Averaging Group Collaboration), Averages of B-Hadron, C-Hadron, and tau-lepton

- properties as of early 2012, [arXiv:1207.1158](https://arxiv.org/abs/1207.1158). Online update at <http://www.slac.stanford.edu/xorg/hfag>.
- [55] T. Abe *et al.*, Belle II technical design report, [arXiv:1011.0352](https://arxiv.org/abs/1011.0352).
- [56] C. Bobeth, M. Gorbahn, T. Hermann, M. Misiak, E. Stamou, and M. Steinhauser,  $B_{s,d} \rightarrow \ell^+ \ell^-$  in the Standard Model, *Phys. Rev. Lett.* **112**, 101801 (2014).
- [57] CMS and LHCb Collaborations, Report No. CMS-PAS-BPH-13-007, 2014; Report No. LHCb-CONF-2013-012, 2014; Report No. CERN-LHCb-CONF-2013-012, 2014.
- [58] R. Aaij *et al.*, Report No. CERN-LHCC-2011-001, 2011; Report No. LHCC-I-018, 2011.
- [59] M. Bona *et al.* (UTfit Collaboration), An improved standard model prediction of  $BR(B \rightarrow \tau \nu)$  and its implications for new physics, *Phys. Lett. B* **687**, 61 (2010). Updated results and plots available at <http://www.utfit.org/UTfit/ResultsSummer2013PostEPS>.
- [60] A. Lenz, Theoretical update of B-Mixing and Lifetimes, [arXiv:1205.1444](https://arxiv.org/abs/1205.1444).
- [61] J. Beringer *et al.* (Particle Data Group Collaboration), Review of particle physics (RPP), *Phys. Rev. D* **86**, 010001 (2012).
- [62] M. Bona *et al.* (UTfit Collaboration), The unitarity triangle fit in the standard model and hadronic parameters from lattice QCD: a reappraisal after the measurements of  $\Delta m_s$  and  $BR(B \rightarrow \tau \nu_\tau)$ , *J. High Energy Phys.* **10** (2006) 081, for updated results and plots.
- [63] M. Baak, M. Goebel, J. Haller, A. Hoecker, D. Kennedy, K. Mönig, M. Schott, and J. Stelzer (The Gfitter Collaboration), Updated status of the global electroweak fit and constraints on new physics, *Eur. Phys. J. C* **72**, 2003 (2012).
- [64] K. G. Chetyrkin, J.H. Kühn, A. Maier, P. Maierhöfer, P. Marquard, M. Steinhauser, and C. Sturm, Charm and bottom quark masses: An update, *Phys. Rev. D* **80**, 074010 (2009).
- [65] Tevatron Electroweak Working Group, CDF Collaboration, and D0 Collaboration, Combination of CDF and D0 results on the mass of the top quark using up to 5.8-fb-1 of data, [arXiv:1107.5255](https://arxiv.org/abs/1107.5255).
- [66] A. J. Buras and J. Girrbach, Towards the identification of new physics through quark flavour violating processes, *Rep. Prog. Phys.* **77**, 086201 (2014).
- [67] N. Carrasco *et al.* (ETM Collaboration), Neutral meson oscillations in the Standard Model and beyond from  $N_f = 2$  Twisted Mass Lattice QCD, *Proc. Sci.*, LATTICE2012 (2012) 105.
- [68] N. Carrasco *et al.* (ETM Collaboration), B-physics from  $N_f = 2$  tmQCD: The Standard Model and beyond, *J. High Energy Phys.* **03** (2014) 016.
- [69] T. Ibrahim and P. Nath, The neutron and the lepton EDMs in MSSM, large  $CP$  violating phases, and the cancellation mechanism, *Phys. Rev. D* **58**, 111301 (1998).